SENRA Academic Publishers, Burnaby, British Columbia
Vol. 2, No. 1, pp. 179-190, 2008
ISSN: 1715-9997

Canadian Journal of pure&applied sciences

THE STUDY OF CONTRACTIBLE BODIES WITH A MICROSENSOR BASED ON THE QUARTZ CRYSTAL RESONATOR

Xiujun Li and *Paul CH Li
Department of Chemistry, Simon Fraser University, Burnaby, BC, Canada, V5A 1S6

ABSTRACT

An acoustic wave method has been employed for the study of contractible bodies using a quartz crystal microsensor. We studied two examples of contractible bodies, namely, the hydrogel polymer and heart muscle cell. First, a hydrogel polymer was formed on the surface of a quartz crystal resonator. This hydrogel polymer can expand under alkaline conditions and contract under acidic conditions. During this process, the elastic properties of the polymer have changed. These modify the acoustic wave propagation of the quartz crystal, and are manifested as changes in the resonant frequency of quartz. The changes have been electrically measured by a network analyzer using the impedance measurement mode. Our results show that the resonant frequency increases when the hydrogel expands, and the frequency decreases while it contracts. The measured parameter can be related to the extent of expansion and contraction. Second, the contraction of the cardiomyocyte (heart muscle cell) has been studied by using the quartz crystal microsensor. When the cell contracts, the microsensor shows decreases in the resonant frequency. Although the contraction mechanisms are different, these frequency results are consistent with those obtained with the hydrogel polymer.

Keywords: quartz crystal microsensor, acoustic wave, impedance measurement, hydrogel, heart muscle cell (cardiomyocyte).

INTRODUCTION

The quartz crystal microsensors have been previously used in the study of biological systems, such as protein adsorption (Yang *et al.*, 1993; Murray and Cros, 1998), immunochemical interactions between antibody and antigen (Kösslinger *et al.*, 1994; Höök *et al*., 1998), and cellular analysis, e.g. endothelial cells (Zhou *et al.*, 2000), osteoblasts (Redepenning *et al*., 1993), viral particles (Cooper *et al.*, 2001), and epithelial (monkey kidney) cells (Gryte *et al*., 1993). In this paper, we employ a similar method to study the motion of contractible bodies, which include the hydrogel polymer bead and the heart muscle cell (or cardiomyocyte). The latter object is a biologically significant example for heart disease studies (Struthers *et al.*, 2004; Bers, 2001).

Currently, several approaches have been used to study the contraction of cardiomyocytes, and these include the measurement of contraction force (Sugi, 1998; Colomo *et al.*, 1994; Brandt *et al.*, 1998), stiffness (Sugi, 1998; Cecchi *et al.*, 1982) and intracellular calcium concentration (Hall *et al.*, 1988; Yu *et al*., 1994; Lindner *et al*., 2002; Garrett and Grisham, 1999). The acoustic wave sensor provides a mechanically simple and label-free method to study muscle cell contraction. This acoustic wave measurement can be achieved by measuring the frequency shift from the natural resonant frequency (eg. 5 MHz) of a quartz crystal after a contractible body was adhered to the gold electrode of the quartz crystal.

By applying an electrical excitation voltage to the quartz crystal via the gold electrodes, periodic mechanical oscillations or acoustic waves in the thickness-shear mode (TSM) will be generated by the converse piezoelectric effect (Salt, 1987b). The waves are confined within the quartz substrate plus any solid film within a short distance of the quartz crystal. In 1965, Sauerbrey's research showed that changes in the resonant frequency were related to the mass of a rigid layer accumulated on the quartz in vacuo (Sauerbrey, 1959). But in liquid solutions, the frequency change is also related to the viscosity and density of the liquid medium, as described by Kanazawa and Gordon (Kanazawa and Gordon, 1985). Yoshimoto *et al.* has recently studied the frequency changes due to periodic change of liquid viscosity and density during an oscillating chemical redox reaction (Yoshimoto *et al.*, 2004).

In the case of the accumulation of a viscoelastic film (e.g. hydrogel or myocytes) on the quartz crystal, the situation becomes much more complicated. To address these issues, Bandey *et al.* (1999), Hayward and Thompson (1998), Bottom (1982), Martin *et al.* (1991), Simpson (1985), Hayward and Chu (1994), Reed *at al*. (1990), and Ferrante *et al*. (1994) indicate that acoustic wave measurement can provide detailed information regarding the interaction between the QCR, the sensing layer and the liquid medium. The resonator can be affected by several factors: mass of a film deposited on the resonator surface; elastic deformation in the film; viscosity of the medium; and changes in the coupling between the film and the medium (Čavić *et al.*, 1999). Any change of one

*Corresponding author email: paulli@sfu.ca

Table 1. Loading effects of water, pH 2, pH 12 solution, and hydrogel monomer mixture

	4 μL water	4 μL pH2	4 μL pH12	1 μL hydrogel
Δf_s /Hz	168 ±5	207 ±6	285 ±8	887 ±3
ΔR /ohm	78±3	97±2	138±3	446 ±1

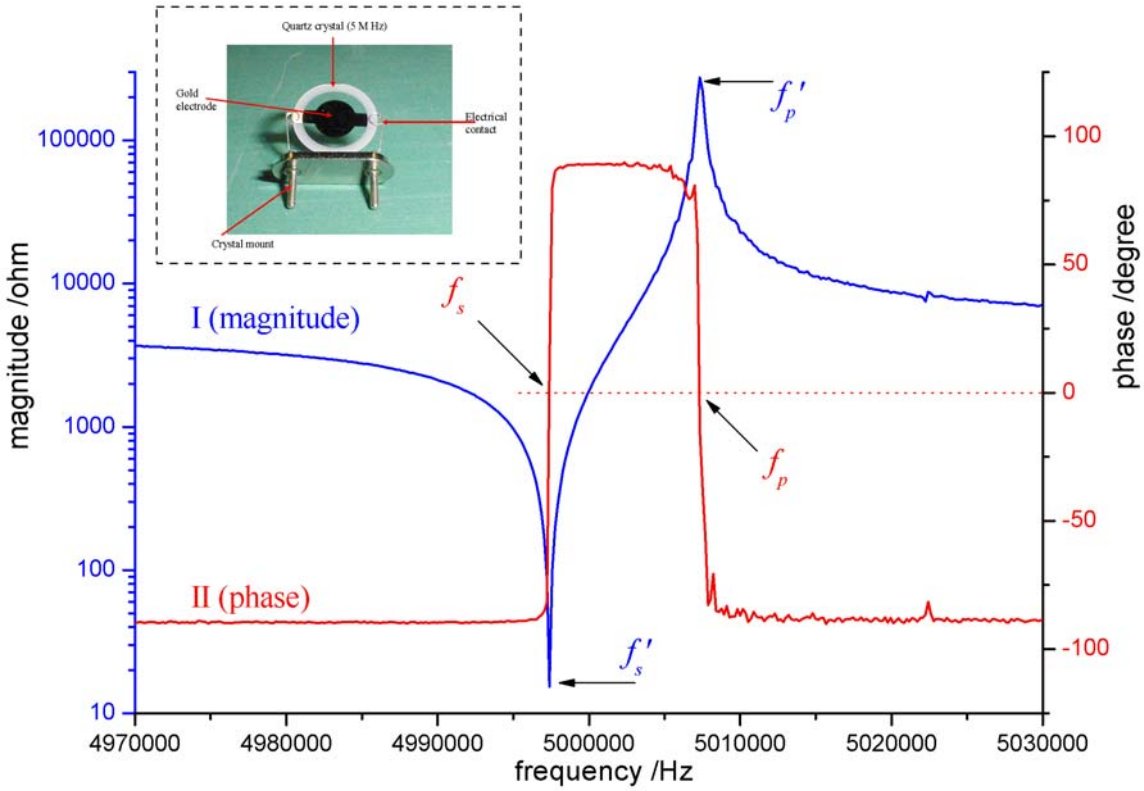

Fig. 1. Magnitude and phase curves of impedance measurement of a QCR in Air and the definition of frequency parameters of f_s, f_p, f_s' and f_p'. The inset is an image of a 5-MHz quartz crystal resonator.

of these factors will cause the corresponding change in the frequency of the microsensor. Recently, Martin *et al.* developed a modified Butterworth-Van Dyke (BVD) model to interpret the coupling between the quartz and viscoelastic film resonances (Martin *et al.*, 2000). Calvo *et al.* (1995) study also showed that the complex impedance would increase when a solid film became viscoelastic upon oxidation (Calvo *et al.*, 2002). Accordingly, any changes in the elastic properties (stiffness) due to the contractible bodies (i.e. the hydrogel or myocytes) will modify the resonant frequency of quartz.

In this paper, we use the quartz crystal microsensor to study two contractible bodies (hydrogel and myocyte), which have the ability to undergo volume and elastic changes in response to the surrounding environment. The hydrogel that was sensitive to pH was formed by the UV-initiated copolymerization of three components (monomers: acrylic acid, 2-hydroxyethyl methacrylate, and cross-linker: ethyleneglycol dimethacrylate), whose polymerization scheme is shown in Scheme 1 (Liu *et al.*, 2000).

Scheme 1. The polymerization reaction initiated by UV to form the hydrogel.

As pH decreases, the hydrogel networks change from charged to neutral because of the reprotonation of the carboxylate groups. Due to less electrostatic repulsion, the hydrogel thus undergoes volume transition to the contracted state (Liu *et al.*, 2000; Beebe *et al.*, 2000). Because of this property, this hydrogel is used as a simplified model of contractible bodies. Thereafter, a biological contractible body- the cardiomyocyte was studied, and its contraction occurred after external Ca^{2+} was introduced to the skinned (or permeated) cell.

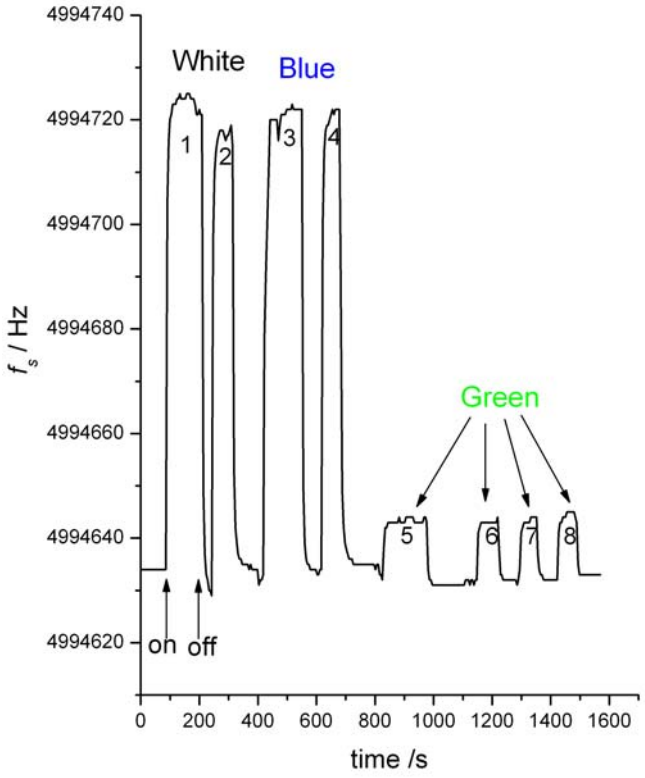

Fig. 2. Thermal effect of the microscope light beam on the f_s measurement of the QCR. At 86s, light was on; At 207s, light was blocked; At 242s, light on; At 313s, light off; At 421s, 620s, 832s, 1150s, 1297s and 1425s, light on. At 551s, 682s, 979s, 1219s, 1353s and 1488s, light off. Plateau 1 and 2, without filters; Plateau 3 and 4, with blue filter; Plateau 5, 6, 7 and 8, with green filter.

Although with different mechanisms, both kinds of contractible bodies showed a similar pattern in the changes in measured parameters of the QCRs upon contraction.

MATERIALS AND METHODS

Reagents

The hydrogel polymer was formed by three monomers: acrylic acid (99%, Aldrich Chemical Company, Inc, Milwaukee, WI), 2-hydroxyethyl methacrylate (99%, Aldrich) and ethylene glycol dimethacrylate (the cross-linker, 98%, Aldrich), and the photoinitiator: 2,2-dimethoxy-2-phenylacetophenone (99%, Aldrich). A pH 2 solution (potassium chloride-hydrochloric acid buffer, Fisher Scientific, Nepean, ON, Canada) and a pH 12 solution of 0.01 M NaOH (97.0%, Merck, Darmstadt, Germany) were used to contract and expand the hydrogel. A 0.1% w/v poly-L-lysine (PLL) solution (Sigma-Aldrich Co., St. Louis, MO) was used for muscle cell attachment on the QCR surface. Sodium dodecyl sulfate (SDS, 99%, Sigma) was obtained from Sigma-Aldrich. All other reagents were of analytical grade.

Instrumentation

Impedance measurement of the AT-cut quartz crystal resonator (5 MHz, International Crystal Manufacturing, Oklahoma City, OK) was carried out by a network/spectrum analyzer (4195A, Hewlett-Packard, now Agilent). An image of a 5-MHz quartz crystal resonator is shown in the inset of Figure 1. Instrument control and data acquisition were performed using a GPIB interface board, and an in-house developed LabVIEW 5.1 virtual instrument (National Instruments, Austin, TX) on a personal computer. An inverted microscope TE300 (Nikon, Mississauga, ON, Canada) with an imaging system (PTI, London, ON, Canada) was used for observation and image capturing. The polymerization of

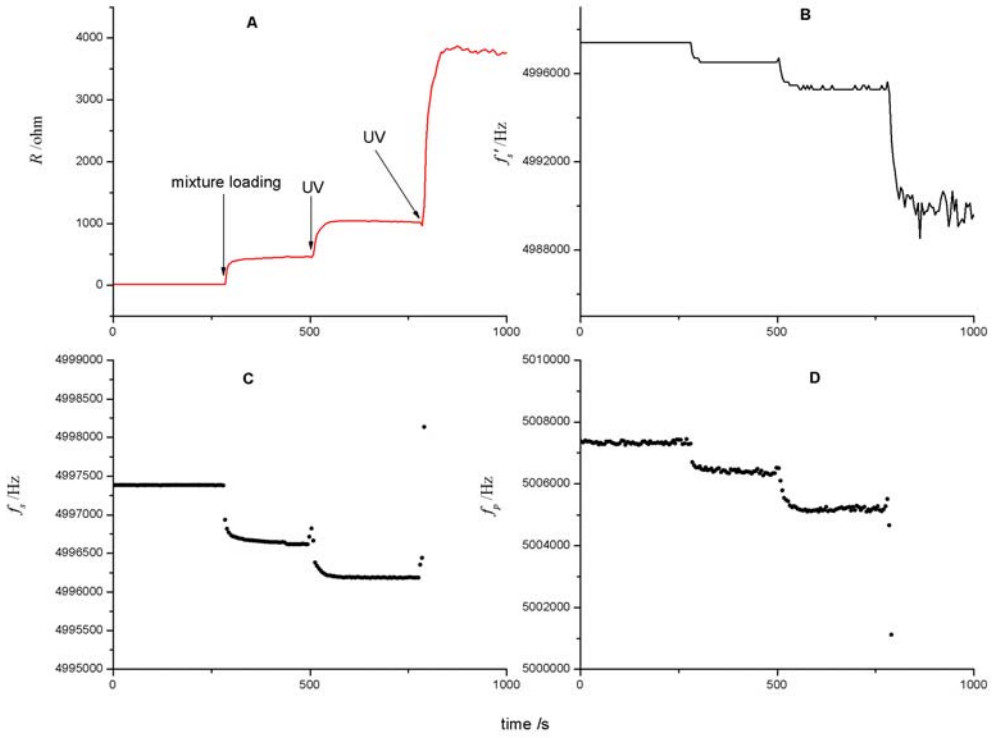

Fig. 3. Monitoring the formation of hydrogel during photo-initiated polymerization. (A) R; (B) f_s'; (C) f_s; (D) f_p. At 284s, 1 µL mixture of monomers was added on QCR; At 508s, UV on 10s. At 790s, UV on 10s.

hydrogel was initiated by a UV curing lamp (HLL400, Dymax, Torrington, CT).

Impedance measurement

Impedance measurement based on network analysis was used because it could provide various resonant frequencies (series and parallel) as well as electrical equivalent circuit parameters (Yang and Thompson, 1993). The impedance magnitude ($|Z|$, curve I in Fig. 1) and impedance phase (Φ, curve II in Fig. 1) of the sensor are continuously computed and registered. Both series resonant frequency, f_s, and parallel resonant frequency, f_p, can be determined from the phase curve during zero-crossing, *i.e.* when Φ= 0 (Salt, 1987a; Rosenbaum, 1988). On the magnitude curve, we also obtain the information such as frequency at minimum impedance, f_s', and frequency at maximum impedance, f_p' (Voelker, 1984). By fitting recorded data to the Butterworth-Van Dyke equivalent electrical circuit which consists of a shunt capacitance, C_0, connected in parallel with a motional arm comprising a capacitor, C_m, an inductor, L_m, and a resistor, R_m (Martin *et al.*, 1991; Hayward and Chu, 1994), the values of the circuit parameters can be calculated from the impedance curves (phase and magnitude).

The procedure for measuring the changes in the frequency and the equivalent circuit parameters is given as follows. After the device was mounted on a holder as we reported before (Li *et al.*, 2003), a frequency sweep (number of points, NOP=401) was first initiated. Then, a delay time of 3 s was introduced to wait for the frequency sweep to complete. A line-cursor function at Φ = 0 was then called. The lower frequency value at which Φ = 0 is f_s, and the higher value corresponds to f_p (see Fig. 1). In addition, the functions of peak-maximum and peak-minimum were called to yield the two frequencies when these maxima occur. In addition, the instrument automatically computed the four equivalent circuit parameters by the phase and magnitude values at the 3-dB points of the series and parallel resonance. Meanwhile, f_s, f_p, f_s', f_p', C_m, L_m, R_m and C_0 were continuously acquired to generate time-course curves in all the eight parameters. Simultaneous optical observation was performed during impedance measurement.

Optical measurement and thermal effect

An optical microscope was employed to examine the contractible bodies during impedance measurement. However, when a light beam of the microscope was

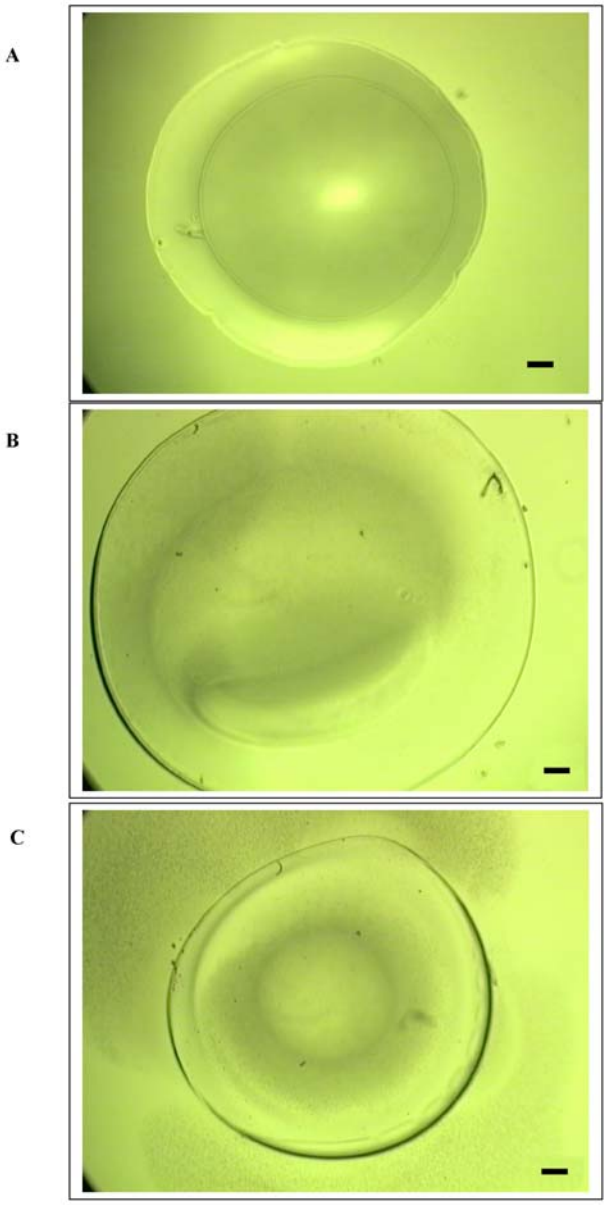

Fig. 4. The image of the expansion and the contraction of a hydrogel bead. (A) cured hydrogel; (B) expanded hydrogel after adding alkali; (C) contracted hydrogel after adding acid. The scale bar represents 100 μm.

turned on, the heat generated from the light caused some changes of the frequency of QCR. Therefore we would like to study the thermal effect as shown in Figure 2. If no light beam was shone on the QCR, the base line was flat which showed that the f_s of QCR was stable under RT. Once a focused beam for microscope observation was shone on it, an increase of frequency of QCR was resulted. But if the beam was turned off, the frequency would go back to its initial level at once. Therefore a high plateau (1) was formed. A second plateau (2) followed when the same procedure was repeated. Different filters (blue-color and green-color filters) were tried to minimize this thermal effect and it was found that green light has less effect on QCR than blue light and white light. Therefore, green light was used in all subsequent experiments when optical observation was performed concurrently with the impedance measurement.

Formation, expansion and contraction of hydrogel

A reaction mixture of a 1:4 mole ratio of acrylic acid to 2-hydroxyethyl methacrylate, 1 wt % ethylene glycol dimethacrylate, and 3 wt % 2,2-dimethoxy-2-phenylacetophenone (photo-initiator) was made. A fixed

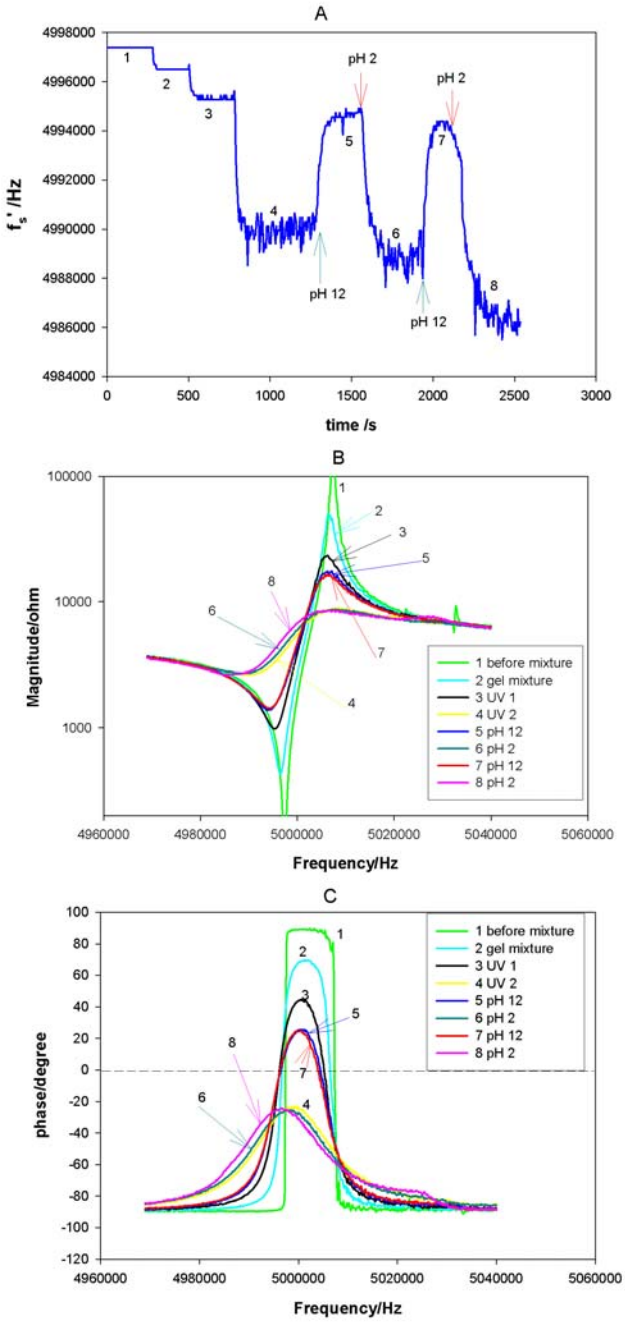

Fig. 5. Monitoring the formation and subsequent expansion and the contraction of hydrogel. (A) f_s'; (B) magnitude comparison; (C) phase comparison. At 1260s, 4 µL pH 12 solution was added; At 1545s, liquid was removed; At 1565s, 4 µL pH 2 solution was added; At 1907s, liquid was removed; At 1931s, 4 µL pH 12 solution was added; At 2097s, liquid was removed; At 2130s, 4 µL pH 2 solution was added. Numbers from 1 to 8 in (A) represent different status of the hydrogel and correspond to different impedance magnitude traces in (B) and phase traces in (C).

amount of the mixture (e.g. 1 µL) was placed on QCR using a micropipette. The gel was then cured using a UV lamp. To expand the hydrogel, a small amount (2-5 µL) of 0.01M NaOH (pH 12) was placed over the hydrogel. The excess solution was removed by suction. To contract the gel, a similar procedure was followed by using the potassium chloride-hydrochloric acid buffer (pH 2). To reduce mass loading, a smaller hydrogel was formed, and a fine capillary tube (OD 360 X ID 249 µm) was used to apply the monomer mixture on the QCR.

Isolation, skinning and attachment of cardiomyocytes

Adult rabbit ventricular cardiomyocytes were obtained from Dr. Tibbits' laboratory in the School of Kinesiology at Simon Fraser University (SFU). The intact cells were

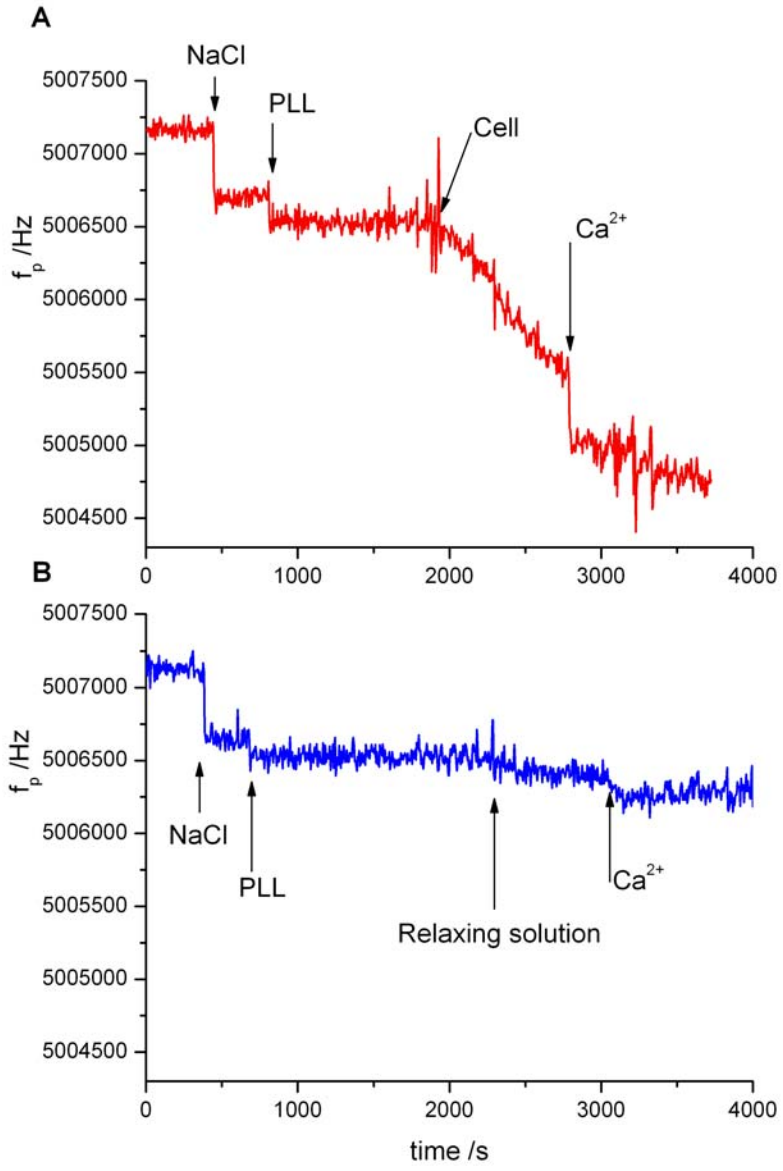

Fig. 6. Cardiomyocyte contraction study induced by calcium on QCR. (A), cell experiment, in which cell suspension in relaxing solution was added; (B), control experiments, in which only relaxing solution was added. Cell experiment conditions: at 438s, 7μL 0.15M NaCl was added; at 804s, 10μL 0.1% (w/v) poly-lysine was added; at 1550s, liquid was removed; at 1936s, 10 μL skinned cell suspension was added; at 2791s, 10 μL 5 mM $CaCl_2$ was added.

freshly isolated from rabbit hearts according to the published procedures and were stored in a relaxing solution (MacDonell *et al.*, 1995). The relaxing solution is a Ca^{2+}-free solution: ATP (adenosine triphosphate) 6.31 mM; EGTA (ethylene glycol-bis(2-aminoethylether)-N,N,N',N'-tetraacetic acid**)** 2.00 mM; $MgCl_2$ 5.70 mM; Kprop (potassium propionate) 156.38 mM; BES (N,N-Bis(2-hydroxyethyl)-2-aminoethanesulfonic Acid) 10.0 mM; Leupeptin 0.1 mM; PMSF (phenylmethylsulfonyl fluoride) 0.1 mM; DTT (dithiothreitol) 1.0 mM.

The skinning (or cell permeation) procedure of the cells was accomplished by incubating the isolated intact cells for 6 minutes with a skinning solution. The skinning solution consisted of 0.1% ultrapure Triton X-100 (Surfact-Amps X-100, Rockford, Illinois) in the relaxing

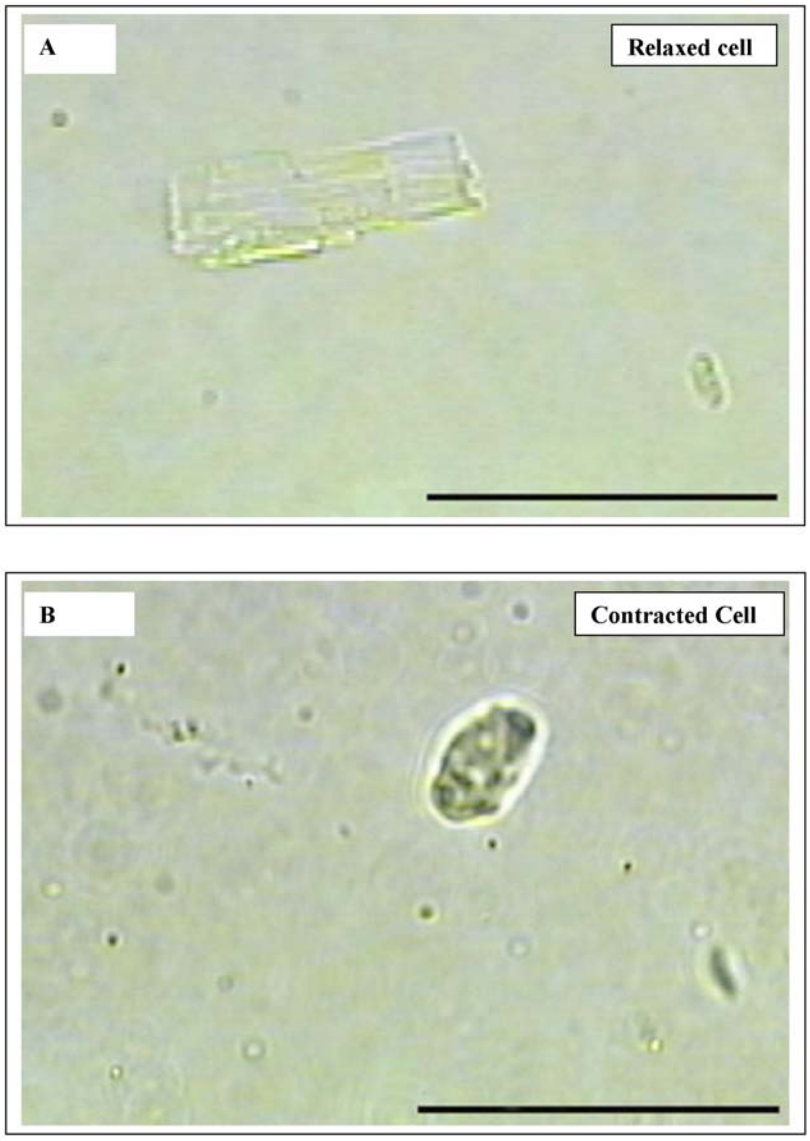

Fig. 7. The contraction process of a skinned rabbit heart muscle cell. (A) a relaxed heart muscle cell after attachment by PLL; (B) the attached heart muscle cell contracted into a round body under the influence of external Ca^{2+} (5mM $CaCl_2$). The scale bar represents 50 μm.

solution. Then the cells were washed with the relaxing solution 2-3 times and stored in ice before use.

The research results from Picart *et al.* show that poly-L-lysine (PLL) can form a positively charged electrolyte layer on QCR (Picart *et al.*, 2001), which will be useful for cell attachment on it. A similar procedure was adopted in this work. First, the gold electrode was cleaned by 0.01M SDS and rinsed with water. Then 0.15 M NaCl, 0.1% w/v poly-L-lysine, solution were sequentially added on the QCR. After about 30 min, a cell suspension was added on the surface for another 15 min for attachment. To induce muscle cell contraction of skinned muscle cells, 5 mM $CaCl_2$ solution was added.

RESULTS AND DISCUSSION

Monitoring the formation of the hydrogel polymer

When the three hydrogel monomers copolymerized as initiated by UV (see Scheme 1), the elasticity and stiffness of the hydrogel film changed. These changes were monitored by the QCR. Figure 3 shows the changes of R, f_s', f_p and f_s (For definitions of these parameters, see the Experimental Section). At 284s, loading of the liquid monomer mixture caused the increase in R (Fig. 3A) and decrease in fs', fs, and f_p (Fig. 3B, 3C and 3D). These changes were caused by the liquid loading effect on the QCR.

Different chemical solutions have different loading effects on the quartz crystal sensor, as reflected in the magnitude of the changes in Δf_s and ΔR. Table 1 shows the different loading effects due to water, pH 2 solution, pH 12 solution and the hydrogel monomer mixture. In all of the aqueous solutions, the same volume of solution (4 μL) was added. As for the hydrogel monomer mixture, only 1 μL was used to avoid excessive damping of the resonator. From Table 1, it is found that water and pH 2 solution have a similar effect of Δf_s and ΔR on the crystal. The pH 12 solution has a slightly greater loading effect on the crystal. The hydrogel monomer mixture has an even greater loading effect. Even 1 μL of the liquid mixture decreased f_s by 887 Hz (~ 5 times as the case of water). This different loading effect is mainly due to two factors, which are liquid density and viscosity, as described by Kanazawa & Gordon's equation (Kanazawa and Gordon, 1985). Since the hydrogel monomer mixture has a greater density and viscosity than others, the mixture will perturb the crystal much more than the other solutions. From Table 1, it can also be seen that the different liquid loading effects caused different R increase. Among these solutions, the liquid monomer mixture caused the greatest increase of 446 ohm. This increase in R was caused by acoustic wave dissipation in the liquid media which is related to the liquid density and viscosity, as reported in the literature (Martin, *et al.*, 1994).

After the first-time UV irradiation (10s) to initiate the polymerization, it caused the decrease of frequency for f_s', f_p and f_s (See Fig. 3). Since the mixture appeared incompletely polymerized after the first UV irradiation, the second irradiation (10s) was applied. Additional decreases of f_s, f_p, and f_s' were observed. These decreases were resulted from the formation of a stiffer polymer film with a greater elasticity. Accompanying these frequency changes, R was increased, which was caused by an increased acoustic energy dissipation in the cured film. In addition, the second one caused much greater changes than the first one, which means that a much greater extent of polymerization or much greater energy dissipation.

Since the QCR was heavily damped after the second-time UV irradiation, the f_s and f_p values were lost because the impedance phase was below zero. But f_s' was still observed. Hence we can still measure f_s' to do further study on the dynamics of polymerization of some polymer materials.

Hydrogel expansion and contraction

After formation of the hydrogel polymer, contraction and expansion of the hydrogel polymer film due to pH change were studied. A circular bead of cured hydrogel was shown in Figure 4A. When the gel is changed to the alkaline condition, the expanded hydrogel bead was observed under the microscope (Fig. 4B). The reverse effect was observed after the contraction of the hydrogel polymer occurred in the acidic state (Fig. 4C).

These expansion and contraction changes of a hydrogel were monitored by the QCR, which were shown in Figure 5. (The formation of this hydrogel polymer has been shown in Fig. 3.) Since f_s and f_p values were lost, only f_s' was shown (See Figure 5. The 0-1000s part of the curve has been shown in Fig. 3B). Figure 5A shows the f_s' changes during the gel formation and subsequent expansion and the contraction of the hydrogel under alkaline and acidic conditions, respectively. When 4 μL pH 12 solution was added at 1260s, an increase of f_s' was observed. This observation cannot be explained by the liquid loading effect because it would lead to frequency decrease. Since the bulk elasticity of the hydrogel decreased when the hydrogel expanded under alkaline conditions, and this effect was greater than the liquid loading effect, we observed an increase, rather than decrease, of frequency.

After removing the alkaline solution and adding pH 2 solution, f_s' decreased due to the contraction of the hydrogel in the acidic environment (Fig. 5A). This similar procedure was repeated to expand and contract the hydrogel, and another plateau was also observed.

The phenomena that the frequency increase or decrease due to the elasticity property change of hydrogel were consistent with the previous research results conducted in hydrogels whose expansions were caused by oxidation rather than a change to a high pH (Calvo *et al.*, 2002; Calvo *et al*., 1995).

To understand more about how the f_s' changed during the expansion and the contraction of the hydrogel, we examined the raw data of the changes in the magnitude curve (Fig. 5B) and the phase curve (Fig. 5C), from which the f_s' values were derived from the minima of the magnitude curves. Here, the curve numbers correspond to the different stages in Figure 5A. In Figure 5B, curve 1 is the magnitude curve before the hydrogel monomer mixture was put on the surface of the QCR. The impedance magnitude decreased when the monomer mixture was loaded on QCR because of the liquid loading effect.

When polymerization occurred as initiated by UV, the impedance decreased more and f_s' (the frequency at the minimum point) shifted to a lower frequency (from curve 2 to 3, and to 4).

After adding the pH 12 solution, the magnitude returned to a higher level and f_s' shifted to higher frequency (curve 5) because of the expansion of hydrogel.

However, when pH 2 solution was added, f_s' decreased again due to the shifting of the magnitude curve (curve 6).

That is the reason why we got a plateau when the hydrogel expanded and contracted. Note that curve 4, 6 and 8 are similar. This is because the hydrogel originally formed was in a lower pH state due to the use of acrylic acid.

For the impedance phase curves, since the maximum phase decreased below zero (i.e. -23.2º) when QCR was heavily damped after polymerization, we cannot get f_s and f_p values. Therefore, f_s' was used to monitor the changes of frequency.

However, we still get some details about the change of phase during these processes by studying the phase comparison (Fig. 5C). It can be found that the liquid loading effect and the polymerization also caused the decrease of the maximum phase and that f_s and f_p decreased as well, due to the curve shifting (from curve 1 to curve 2, 3, 4). One interesting observation was that after polymerization, the phase decreased to below zero (-23.2º). But when the hydrogel expanded, the expansion caused the phase to increase above zero (25.5º). The expansion caused a large change of the phase. This change would be manifested as discontinued changes if f_s and f_p were monitored.

From these results, it can be seen that the contraction of a contractible body (here it is the hydrogel polymer) will cause f_s' to decrease, but the expansion of the contractible body will lead to the increase of f_s'. This observation provides us more information to carry on further study on other contractible bodies, such as cardiomyocytes, the heart muscle cells.

Monitoring the contraction of heart muscle cells

The contraction of heart muscle cells are preceded by the increase of intracellular calcium concentration (Garrett and Grisham, 1999) which is due to the flow of Ca^{2+} through calcium channels on the cells' membranes upon stimulation. On the other hand, if the cell membrane was permeated or skinned, cell contraction can also be initiated by a free flow of external calcium ions into the cell through the skinned cell membrane.

The contraction of heart muscle cells were studied by the QCR. Since the damping effect of the cell suspension on the QCR is smaller, the phase appears to be always above zero. Therefore, the f_s and f_p values could be extracted. During experiments, it was found that f_p is more sensitive to cell contractions as similarly observed previously (Li *et al.*, 2003), and so f_p was used to depict the frequency changes due to cell contractions, as shown in Figure 6. Figure 6A is the cell experiment and Figure 6B is the control experiment (without cells). The common features in them are that the first two frequency decreases are due to the loading of NaCl and PLL solutions for cell adhesion purpose. The third decrease was caused by loading of cells. The adhesion of cells caused a gradual decrease in f_p, which was not seen in the control experiment without cells.

After the calcium solution was added, there was a sudden decrease in f_p even before it reached a steady value (Fig. 6A). This change was attributed to the contraction of cells as induced by influx of external calcium. In comparison, there was a smaller decrease in f_p due to the liquid loading effect (Fig. 6B).

To confirm cell contraction due to external calcium, Figure 7 shows the appearance of a skinned heart muscle cell attached on a glass slide before and after the addition of external calcium (5mM in relaxing solution). Before putting the cells solution on the glass slide, the slide has been treated with 0.1% w/v poly-L-lysine solution in order to promote the attachment of the cells on the slide so that we can keep track of the cell and see its contraction. If we did not use the treated slide, when we added the calcium solution to the cell on the slide, the cell as observed by microscopy would be flushed away.

These preliminary data show that the contraction of heart muscle cells would also cause the frequency decrease. Such a frequency decrease has similarly been observed in the hydrogel contraction experiment.

CONCLUSIONS

This work demonstrated a label-free method to study the contraction of contractible bodies with a microsensor based on the quartz crystal resonator. We studied two examples of contractible bodies, namely hydrogel polymer and heart muscle cell (cardiomyocyte). Our results show that the resonant frequency increases when the hydrogel expands, and the frequency decreases while it contracts. For heart muscle cells, when they contracted, the microsensor showed decreases in resonant frequency. The preliminary results are consistent with those obtained with the hydrogel polymer.

Further work includes device characterization plus mathematical correlation of the acoustic frequency changes with the cell contraction parameters. Thereafter, this microsensor could be used to screen heart disease drugs based on the extent of how these drugs alter muscle cell contraction.

ACKNOWLEDGEMENTS

Financial support from CFI, BCKDF, CIHR development grant is gratefully acknowledged. We are also grateful to Dr. Glen F. Tibbits and co-workers (Bo Liang, Xiaoye (Helen) Sheng, Jingbo Huang and Haruyo Kashihara) for providing the muscle cells and useful advice, as well as Lung Wong for Labview programming.

REFERENCES

Bandey, HL., Martin, SJ., Cernosek, RW. and Hillman, AR. 1999. Modeling the Responses of Thickness-Shear Mode Resonators under Various Loading Conditions. Anal. Chem. 71: 2205-2214.

Beebe, DJ., Moore, JS., Bauer, JM., Yu, Q., Liu, RH., Devadoss, C. and Jo, B. 2000. Functional hydrogel structures for autonomous flow control inside microfluidic channels. Nature. 404: 588-590.

Bers, DM. (ed.). 2001. Excitation-Contraction Coupling and Cardiac contractile Force. Kluwer Academic Publishers, Dordrecht / Boston /London, p. 316.

Bottom, VI. 1982. Introduction to Quartz Crystal Unit Design. Van Nostrand Reinhold, New York, USA.

Brandt, PW., Colomo, F., Piroddi, N., Poggesi, C. and Tesi, C. 1998. Force regulation by Ca2+ in skinned single cardiac myocytes of frog. Biophys. J. 74: 1994-2004.

Calvo, EJ., Danilowicz, C. and Etchenique, R. 1995. Measurement of viscoelastic changes at electrodes modified with redox hydrogels with a quartz crystal device. J. Chem. Soc. Faraday Trans. 91: 4083-4091.

Calvo, EJ., Forzani, ES. and Otero, M. 2002. Study of Layer-by-Layer Self-Assembled Viscoelastic Films on Thickness-Shear Mode Resonator Surfaces. Anal. Chem. 74: 3281-3289.

Čavić, BA., Hayward, GL. and Thompson, M. 1999. Acoustic waves and the study of biochemical macromolecules and cells at the sensor-liquid interface. Analyst. 124: 1405-1420.

Cecchi, G., Griffiths, PJ. and Taylor, S., 1982. Muscular contraction: kinetics of crossbridge attachment studied by high-frequency stiffness measurements. Science. 217: 70-72.

Colomo, F., Poggesi, C. and Tesi, T. 1994. Force responses to rapid length changes in single intact cells from frog heart. J. Physiol. 475: 347-350.

Cooper, MA., Bultsev, FN., Minson, T., Ostanin, VP. Abell, C. and Klenerman, D. 2001. Direct and sensitive detection of a human virus by rupture event scanning. Nat. Biotechnol. 19: 833-837.

Ferrante, F., Kipling, AL. and Thompson, M. 1994. Molecular slip at the solid-liquid interface of an acoustic-wave sensor. J. Appl. Phys. 76: 3448-3462.

Garrett, RH. and Grisham, CM. 1999. Biochemistry. Saunders College Publishing, New York, 2nd edition, p.540.

Gryte, DM., Ward, MD. and Hu,WS. 1993. Real-time measurement of anchorage-dependent cell adhesion using a quartz crystal microbalance. Biotechnol. Prog. 9: 105-108.

Hall, JS., Kordidis, KA. and Maskevich, DL. 1988. Fluorometric calcium measurement. Nature. 331: 729-729.

Hayward, GL. and Chu, GZ. 1994. Simultaneous measurement of mass and viscosity using piezoelectric quartz crystals in liquid media. Anal. Chim. Acta. 288: 179-185.

Hayward, GL. and Thompson, M. 1998. A transverse shear model of a piezoelectric chemical sensor. J. Appl. Phys. 83: 2194-2201.

Höök, F., Rodhal, M., Brzezinski, P. and Kasemo, B. 1998. Energy Dissipation Kinetics for Protein and Antibody-Antigen Adsorption under Shear Oscillation on a Quartz Crystal Microbalance. Langmuir. 14: 729-734.

Kanazawa, KK. and Gordon, JG. 1985. The oscillation frequency of a quartz resonator in contact with liquid. Anal. Chim. Acta. 175: 99-105.

Kösslinger, C., Drost, S., Aberl, F. and Wolf, H. 1994. Quartz crystal microbalance for immunosensing. Fresenius J. Anal. Chem. 349:349-354.

Li, PCH., Wang,W. and Parameswaran, M. 2003. An acoustic wave sensor incorporated with a microfluidic chip for analyzing muscle cell contraction. Analyst. 128: 225-231.

Lindner, M., Brandt, MC., Sauer, H., Hescheler, J., Böhle, T. and Beuckelmann, DJ. 2002. Calcium sparks in human ventricular cardiomyocytes from patients with terminal heart failure. Cell Calcium. 31: 175-182.

Liu, RH., Yu, Q., Bauer, JM., Jo, B., Moore, JS. and Beebe, DJ. 2000. Micro Total Analysis Systems 2000, Proceedings of the μTAS Symposium. Enschede, Netherlands, p. 375.

MacDonell, KL. Tibbits, GF. and Diamond, J. 1995. cGMP elevation does not mediate muscarinic agonist-induced negative inotropy in rat ventricular cardiomyocytes. Am. J. Physiol. 269: H1905-H1912.

Martin, SJ., Bandey, HL. and Cernosek, RW. 2000. Equivalent-Circuit Model for the Thickness-Shear Mode Resonator with a Viscoelastic Film Near Film Resonance. Anal. Chem. 72: 141-149.

Martin, SJ., Frye, GC. and Wessendorf, KO. 1994. Sensing liquid properties with thickness-shear mode resonators. Sens. Acta A. 44: 209-218.

Martin, SJ., Granstaff, VE. and Frye,GC. 1991. Characterization of a quartz crystal microbalance with simultaneous mass and liquid loading. Anal. Chem. 63: 2272-2281.

Murray, BS. and Cros, L. 1998. Adsorption of β-lactoglobulin and β-casein to metal surfaces and their removal by a non-ionic surfactant, as monitored via a

quartz crystal microbalance. Colloids Surf. B: Biointerfaces. 10:227-241.

Picart, C., Lavalle, Ph., Hubert, P., Cuisinier, FJG., Decher, G., Schaaf, P., Voegel, JC. 2001. Buildup Mechanism for Poly(L-lysine)/Hyaluronic Acid Films onto a Solid Surface. Langmuir. 17: 7414-7424.

Redepenning, J., Schlesinger, TK., Mechalke, EJ., Puleo, DA. and Bizios, R. 1993. Osteoblast attachment monitored with a quartz crystal microbalance. Anal. Chem. 65:3378-3381.

Reed, CE., Kanazawa, KK. and Kaufman, JH. 1990. Physical description of a viscoelastically loaded AT-cut quartz resonator. J. Appl. Phys. 68: 1993-2001.

Rosenbaum, JF. 1988. Bulk Acoustic Wave Theory and Devices. Artech House, Boston, p. 413.

Salt, D. 1987a. HyQ Handbook of Quartz Crystal Devices. Van Nostrand Reinhold, England, UK, p. 101.

Salt, D. 1987b. HyQ Handbook of Quartz Crystal Devices. Van Nostrand Reinhold, England, UK, p. 47.

Sauerbrey, GZ. 1959. Verwendung von Schwingquarzen zur Wägung dunner Schichten und zur Mikrowägung. Z. Phys. 155: 206.

Simpson, RL. 1985. PhD Thesis, University of Washington, USA.

Struthers, R., Savik, K. and Hodge, FS. 2004. American Indian Women and Cardiovascular Disease: Response Behaviors to Chest Pain. J Cardiovasc Nurs. 19: 158-163.

Sugi, H. 1998. Current Methods in Muscle Physiology. Advantages, Problems and Limitations, Oxford University Press, New York, USA.

Voelker, KM. 1984. 6th Ann. Quartz Devices Conf., Kansas City, USA, p. 42.

Yang, M. and Thompson, M. 1993. Multiple chemical information from the thickness shear mode acoustic wave sensor in the liquid phase. Anal. Chem. 65: 1158-1168.

Yang, M., Chung, FL. and Thompson, M. 1993. Acoustic network analysis as a novel technique for studying protein adsorption and denaturation at surfaces. Anal. Chem. 65:3713-3716.

Yoshimoto, M., Shirahama, H., Kurosawa, S. and Naito, M. 2004. Periodic change of viscosity and density in an oscillating chemical reaction. J. Chem. Phys. 120: 7067-7070.

Yu, Z., Tibbits, GF. and Maneill, JH. 1994. Cellular functions of diabetic cardiomyocytes: contractility, rapid-cooling contracture, and ryanodine binding. Am. J. Physiol. 266: H2082-H2089.

Zhou, T., Marx, KA., Warren, M., Schulze, H. and Braubut, S.J. 2000. The quartz crystal microbalance as a continuous monitoring tool for the study of endothelial cell surface attachment and growth. Biotechnol. Prog. 16:268-277.